

2-5-3 Calibration of Horn Antenna

Iwao NISHIYAMA, Kojiro SAKAI, Tsutomu SUGIYAMA, Kouichi SEBATA, and Katsumi FUJII

This paper describes the calibration method of the pyramidal standard horn antenna for the frequency band from 1 to 18 GHz. NICT performs the calibration of horn antennas by the three-antenna method. We introduce the three-antenna method and show the calibration results of horn antennas. In addition, we describe the detail of the calibration uncertainties.

1 Introduction

NICT has been providing calibration services of the measurement instruments used for testing radio equipment, according to Article 24-2 of the Radio Law. The Law designates the following six types of measurement equipment as the targets of calibration; frequency meter; spectrum analyzer; electric field strength meter; RF power meter; voltammeter; and standard signal generator. The Law provides no particular direct stipulations on antennas. However, because the correct electric field is required for the precise calibration of the electric field meter, calibrated antennas must be used. NICT has been providing antenna calibration services mainly for the following types of antennas: 9 kHz to 30 MHz loop antennas, 30 to 1,000 MHz dipole antennas, and 1 to 40 GHz horn antennas.

In this paper, we will present descriptions of 1 to 18 GHz horn antenna calibration. In 1993, we started our horn antenna calibration services for 1 to 5 GHz standard pyramidal horn antennas [1], expanding the serviceable frequency range in 1998 to 18 GHz. Along with the provision of calibration service, we have been studying uncertainty analysis [2] in detail. Furthermore, since 2009, our services have been available for the frequency range of up to 40 GHz. We will introduce general descriptions on our service of the frequency range of up to 18 GHz among our currently available services for horn antennas, and then we will report the details of the uncertainty in our current calibration system.

2 Principles of antenna calibration

The following three methods are generally used for antenna calibration: (1) Reference Method, where calibration values are obtained by making multiple measurements

on the standard antenna and the antennas under calibration by alternating them to compare the measurements; (2) Standard Electric Field Method, where calibration values are determined by using the electric field strength at the position of the antenna under calibration which is estimated from the transmitted electric field strength; (3) Three-antenna method, where the gains of the individual three antennas are determined by making measurements on the combination of two antennas out of those antennas. The three-antenna method (hereinafter written as “TAM”) has such an advantage over the other two methods that it is available for calibrating any type of antenna if the antenna can be used for transmitting and receiving. In addition, the method gives calibration values with sufficient accuracy relatively easily when the measurements are executed in a fully anechoic room which can provide a space that can be treated as a free space. Consequently, we have employed the TAM for calibrating horn antennas.

The TAM is based on the Friis transmission equation [3]. When a measurement is made on a combination of two antennas—out of the three antennas #1, #2, and #3—placed away from each other at a distance d as shown in

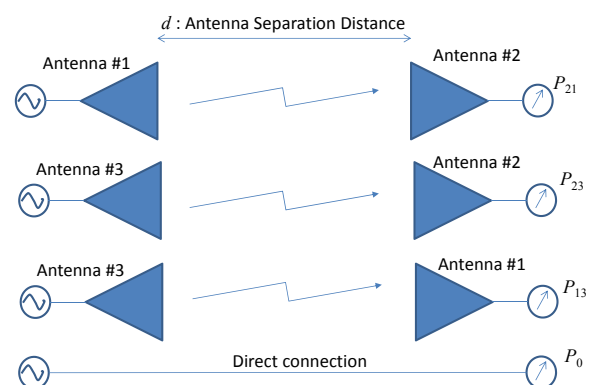


Fig. 1 Three-antenna method (TAM)

Fig. 1, when denoting the reception powers as P_{21} , P_{23} , and P_{13} , respectively, for the combination of antenna #1-#2, #3-#2, and #3-#1, also denoting the direct receiving power without antennas as P_0 , we can determine the antenna gains G_1 , G_2 or G_3 of the individual antennas #1, #2, and #3, under a condition where the impedance of measurement instruments are matched, by using Equation (1), (2) or (3)

$$G_1 = \frac{4\pi d}{\lambda} \sqrt{\frac{P_{21}P_{13}}{P_{23}P_0}} \quad (1)$$

$$G_2 = \frac{4\pi d}{\lambda} \sqrt{\frac{P_{21}P_{23}}{P_{13}P_0}} \quad (2)$$

$$G_3 = \frac{4\pi d}{\lambda} \sqrt{\frac{P_{13}P_{23}}{P_{21}P_0}} \quad (3)$$

where the λ is the frequency of the signal used for the measurement, and the antenna separation d is identical for any of the antenna combinations.

We can determine the gains more accurately if the antenna separation distance is identical to the distance between the antenna phase centers for any antenna combination.

Antenna gains are regularly expressed in decibel values, and so are the measurements of receiving power; for instance, the antenna gain G^{dB} of #1 antenna is expressed in dB by Equation (4).

$$G_1^{dB} = 10 \log_{10} \left(\frac{4\pi d}{\lambda} \right) + \frac{1}{2} (P_{21}^{dB} + P_{13}^{dB} - P_{23}^{dB} - P_0^{dB}) \quad (4)$$

3 Calibration system

In Figure 2, we show the block diagram of calibration system. The internal shield of the large fully anechoic room where calibration is carried out has the dimensions of 28.5 m (L), 17.0 m (W) and 11.7 m (H). Antennas are mounted on Bakelite antenna stands placed on polystyrene foam blocks. Antenna stands are equipped with fine tuning mechanisms for adjusting antenna height, azimuth angle, and elevation angle, enabling easy setting of antennas exactly face-to-face. The standard pyramidal horn antenna, which covers the frequency range of 1 to 18 GHz by eight bands, is designed so that its aperture plane is always in the fixed position for any of the eight bands. The vector network analyzer, working as a transmitter/receiver, is connected to the antennas via low-loss coaxial cables whose antenna ends are connected to the antennas through 6 dB fixed attenuators for reducing the effects of multiple reflections that will be generated when a mismatching occurs.

4 Calibration results

In Figure 3, we show instances of our horn antenna gain calibrations, where we show the trends in the gains measured for the calibrations we conducted in each year. In the figure, the measurement years are lined along the horizontal axis, and the calibration results, which are shown as antenna gains in dBi, are plotted in the vertical

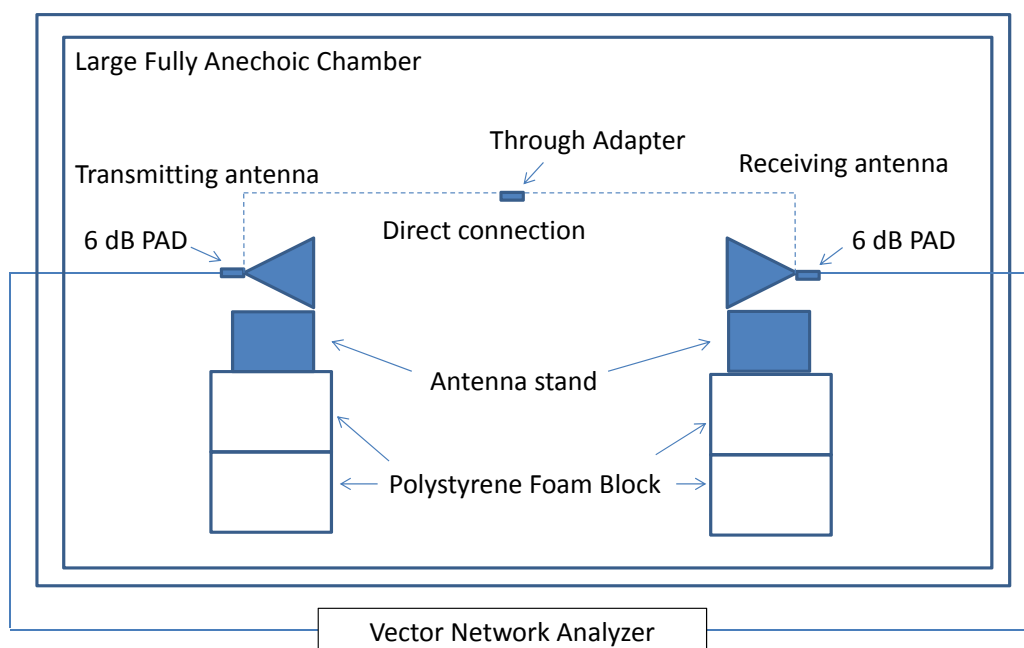


Fig. 2 Measurement system block diagram

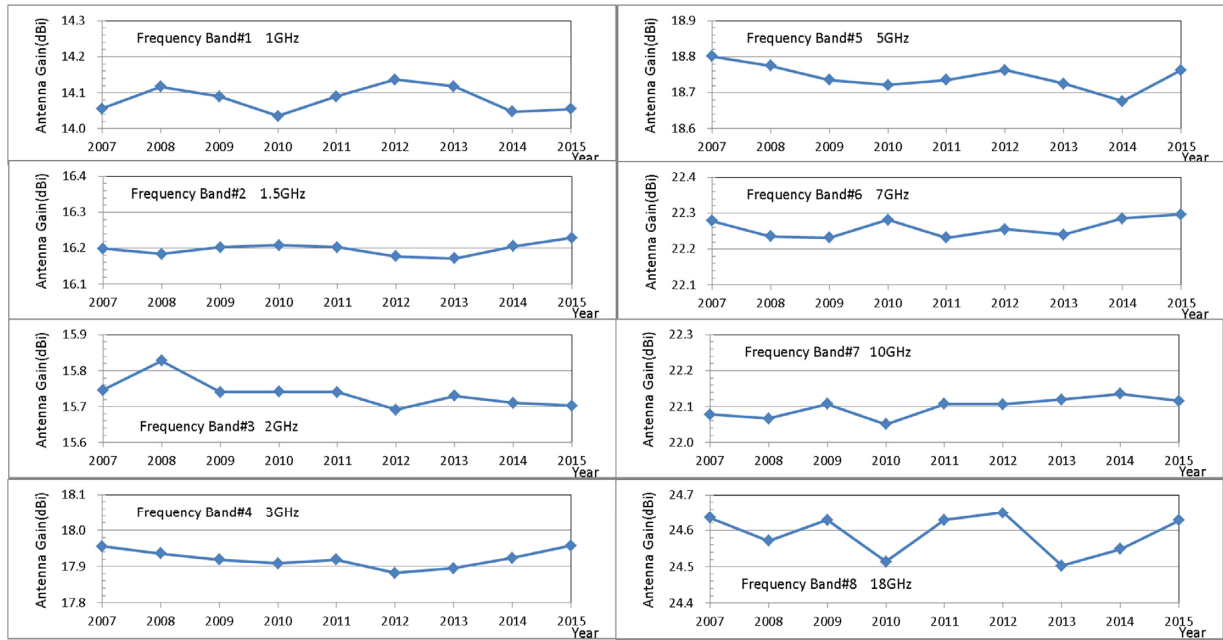


Fig. 3 Trends in calibrated antenna gains

axis direction. The frequency shown in each of the plots is the representative frequency of the frequency band. The maximum gain deviation for the 18 GHz band, where the deviation is larger than in any other band, is 0.15 dB. In Figure 4, we show the calibrated gains for the band #8 (12 to 18 GHz) in the three years from 2013 to 2015, where we can show that the deviations are always within a range narrower than 0.1 dB for any frequency in the band.

5 Uncertainty

We determine gains using Equation (4). Then the standard uncertainty U can be calculated using Equation (5), which combines the uncertainty in the antenna separation distance measurement U_d , the uncertainty in the receiving power measurement U_R , and the uncertainty in direct power connection measurements U_{R0} .

$$U(dB) = \sqrt{\{u_d(dB)\}^2 + \frac{3}{2}\{u_R(dB)\}^2 + \frac{1}{2}\{u_0(dB)\}^2} \quad (5)$$

Note that we calculated the uncertainty in the receiving power measurement using the worst data across all frequency bands, not within each frequency band. On the other hand, while the wavelength λ is included in Equation (4), we neglected the uncertainty in wavelength, because the frequency stability of the vector network analyzer we used (Agilent Technologies, Model E8362B) is ± 1 ppm—much smaller than those derived from other uncertainty sources. In the following subsections, we will individually discuss the causes of uncertainty.

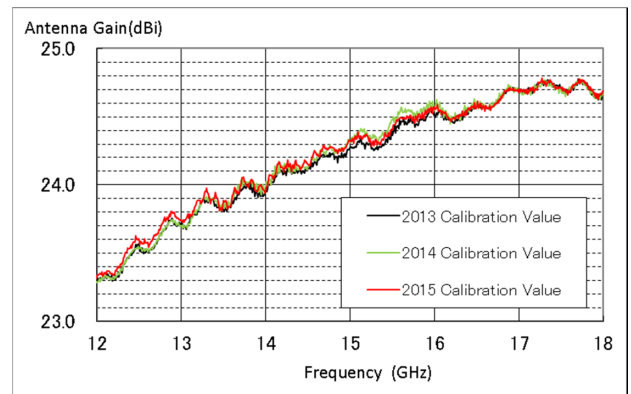


Fig. 4 Band #8 calibration data

5.1 U_d : Uncertainty in antenna separation distance

We will consider two factors as possible factors causing the uncertainty in antenna separation distance: uncertainty in the distance measurement, and uncertainty in the antenna phase center determination.

(1) u_{d1} : Uncertainty in Antenna Separation Distance Measurement

We determined the antenna separation distance by making distance measurements after installing antennas with a laser rangefinder of the accuracy of 1 cm or less ($\Delta d = 1$ cm). We used Equation (6) for estimating u_{d1} , obtaining the uncertainty of 0.003 dB with a rectangular probability distribution by applying $d = 15$ m for an antenna separation distance d , which is the actual measurement.

$$u_{d1}(dB) = \left| 10 \log_{10} \left(1 - \frac{\Delta d}{d} \right) \right| \quad (6)$$

Note that we have neglected the variations in the antenna separation distances for various combinations of antennas, because the distance variation is estimated as less than 1 mm, which is negligibly smaller than the measurement accuracy of antenna separation distance Δd .

(2) u_{d2} : Uncertainty in the position of antenna phase center

By definition, the antenna phase center of a horn antenna is the point of the imaginary point wave source that we can use in place of the horn antenna under the far-field condition. Therefore, in the TAM, by assuming that the antenna separation distance is identical to the distance between the antenna phase centers, we can make more accurate calibrations. However, because a lot of work will be required for determining the antenna phase center position, such methods will not be applicable to actual calculation business operations. Instead, we employed a procedure as shown in Fig. 5 to determine the antenna separation distance in our calibration operations, where we assume that the phase center exists on a middle point of the pyramidal horn length L .

However, the actual phase center possibly exists anywhere in between the aperture and the deepest point of the horn; therefore, the antenna separation distance has an uncertainty of a range of $d-L$ to $d+L$. We can estimate the uncertainty due to such uncertainty in the phase center position by assigning L to Δd in Equation (6), obtaining an estimation of the uncertainty of 0.08 to 0.13 dB, according to the sizes of the antenna for the individual bands, with a rectangular probability distribution.

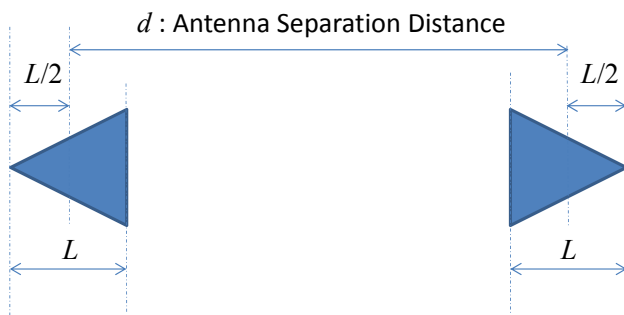


Fig. 5 Phase center and antenna separation distance

5.2 U_R : Uncertainty of reception power measurement

We can generally assume that the following three factors contribute to the uncertainty in receiving power measurement: the uncertainty in the measurement system, the uncertainty in the antenna setting and the uncertainty in the measurements.

5.2.1 Uncertainty in measurement system

Below, we introduce our discussion on the following four factors leading to the uncertainty in the measurement system: the uncertainty due to cable bending, the uncertainty due to measurement instrument instability, the uncertainty due to the nonlinearity in the measurement instrument characteristics and the uncertainty due to the limitation in the indicator resolution of measurement instrument. Note, we assume that each of the factors has a rectangular probability distribution, which will produce standard uncertainty when divided by $\sqrt{3}$.

(1) u_{R1} : Uncertainty due to coaxial cable bending

While cabling is done usually with a sufficient margin, it is difficult to avoid cable bending around the connections to the horn antennas. For the purpose of assessing the actual impacts of cable bending, we made observations of how much level variation occurred while bending a cable, reaching a conclusion that the level variation is 0.03 dB or less even at the highest frequency band.

(2) u_{R2} and u_{R3} : uncertainty due to measurement instrument instability

We have been using the vector network analyzer in our operation following the procedure of warming up the instrument sufficiently before starting measurements. However, a time duration or temperature variation can cause slight level variations. We conducted observations of the vector network analyzer for assessing its stability, obtaining the following results: the level variation was less than 0.05 dB due to time shift, and less than 0.03 dB due to room temperature variation in the air conditioning.

(3) u_{R4} : Uncertainty due to the Non-linearity in Measurement Instrument

We conducted the non-linearity observations using RF attenuators which are traceable back to the National Standards, obtaining the result that the non-linearity is less than 0.05 dB.

(4) u_{R5} : Uncertainty due to Measurement Instrument

Indication Resolution

The finest indication step of the measurement instrument is 0.01 dB; so, we are to assume the uncertainty of its half, 0.05 dB.

5.2.2 Uncertainty due to antenna setting

We estimated the uncertainty due to the antenna setting by considering the following factors: uncertainty in far-field condition and uncertainty in axis alignment. We studied the uncertainty in axis alignment through making breakdowns into the uncertainty in horizontal position, vertical position, azimuth angle, elevation angle and polarization angle. Assuming that each of the factors has a rectangular probability distribution, the standard uncertainties can be obtained using $\sqrt{3}$ as a divisor.

(1) u_{R6} : uncertainty in far-field conditions

In a condition where the antenna separation distance is finite, the wave-front of amplitude arriving at the aperture surface of the antenna under calibration is non-uniformly distributed, leading to errors in measurement. We treat as the uncertainty in far-field condition. Denoting the wavelength λ and the maximum dimension of the antenna aperture D —for a pyramidal horn antenna, the diagonal length—, we can calculate, by using Equation (7), the distance between the antenna apertures R that produces an error of 0.05 dB or less.

$$R \geq \frac{2(D+D)^2}{\lambda} \quad (7)$$

The condition of Equation (7) is satisfied for the antenna separation distance is satisfied only in Band 1, 3 or 5. The approximate value of such uncertainty in the far-field condition can be estimated using Equation (8) [4].

$$u_{R6}(dB) = 12.8 \cdot \left\{ \frac{(D+D)^2}{8R\lambda} \right\} \quad (8)$$

(2) u_{R7} , u_{R8} , u_{R19} , and u_{R11} : uncertainty due to antenna alignment

We conducted antenna alignments by the following procedure: placing a laser generator at the middle point of the line connecting the aperture centers of the antennas facing each other, and adjusting the antenna stands so that each of the center lines of the antenna stands coincides with the vertical plain and the horizontal plain that are indicated by the laser generator. Each antenna is mounted on the stand by inserting the Bakelite plate on which the antenna is attached into one of the slits opened on the stand according to the sizes of the antennas for different frequency bands. While having observed in our calibration

operations so far almost no significant errors in axis alignment, we assumed that the following errors exist in the axis alignment: 1 cm in the horizontal or vertical direction; 1 degree in the angle of azimuth, elevation or polarization. We then applied these error values to antenna of different shapes, converted them into signal strength values, and interpreted them as input uncertainties.

5.2.3 Uncertainty derived from measurement

With regard to the uncertainty derived from measurements, we will discuss the uncertainties due to the variability in the signal-to-noise ratio, caused by the reflections from the inside of fully anechoic room environment, due to mismatching, or due to measurement variability.

(1) u_{R12} : uncertainty due to the variability in signal-to-noise ratio

While the S/N ratio is generally getting worse as the frequency goes higher, in our cases it remains around 50 dB in the highest frequency band of 18 GHz. We estimated the uncertainty in the S/N ratio by using Equation (9) with an assumption that the S/N ratio distributes by a normal probability distribution.

$$u_{R12}(dB) = \left| 20 \log_{10} \left\{ 1 - 10^{\left(\frac{SN}{20} \right)} \right\} \right| \quad (9)$$

(2) u_{R13} : uncertainty due to the reflection from the inside of fully anechoic room environment

The TAM principally considers direct waves in a free space; therefore, it may produce a result with uncertainties if apply an environment where reflections from environments are non-negligible. For assessing such impacts of reflections, we conducted a test where we made measurements on different antenna separation distances, obtaining the following results: the worst impact of 0.09 dB was observed in the highest frequency band #8.

(3) u_{R14} : uncertainty due to mismatching

With regard to the uncertainty due to mismatching, we made measurements, as shown in Fig. 6, of Γ_{A1} , the antenna reflection coefficient; Γ_{AT} , the coefficient at the end of transmitting cable; and Γ_{R} , the coefficient at the receiving cable. Then, we applied those coefficients to Equation (10) to determine the uncertainty [5].

$$u_{R14}(dB) \approx 8.686 \cdot \sqrt{|\Gamma_T|^2 \left(|S_{D11}|^2 + |\Gamma_{A1}|^2 \right) + |\Gamma_R|^2 \left(|S_{D22}|^2 + |\Gamma_{A1}|^2 \right) + |\Gamma_T|^2 |\Gamma_R|^2} \quad (10)$$

where the S_{D11} and S_{D22} are the S_{11} and S_{22} of the through adapter, respectively. The value of uncertainty is estimated by applying the worst values of the S_{D11} and S_{D22} in each frequency band.

The uncertainty due to mismatching is assumed to distribute according to a U-shape probability distribution, so it has a division of $\sqrt{2}$.

(4) u_{R15} : Uncertainty due to repeatability in measurements

Usually, we repeat measurement three times for three horn antennas of each band. We estimated the repeatability in measurements by using the experimental deviation of the measured values. We determined the standard deviation of the averaged value by dividing the experimental standard deviation by $\sqrt{3}$, the square root of the measurement repetition count.

5.3 U_{R0} : Uncertainty in direct connection power measurement

We composed the uncertainty in direct connection power measurement by adding the uncertainty in attenuation due to the through adapters to the uncertainty in measurement system which was described in 5.2.1. We confirmed that the attenuation of the through adapter is 0.1 dB or less in the frequency range of 1 to 18 GHz through the measurements using the vector network analyzer. The uncertainty distributes according to a rectangular probability distribution with ± 0.1 dB.

5.4 Uncertainty budget

In Table 1, we show the uncertainty budget, where, for the uncertainties due to S/N, mismatching, and repeatability, we used their worst values in the individual frequency bands. We finally obtained the expanded

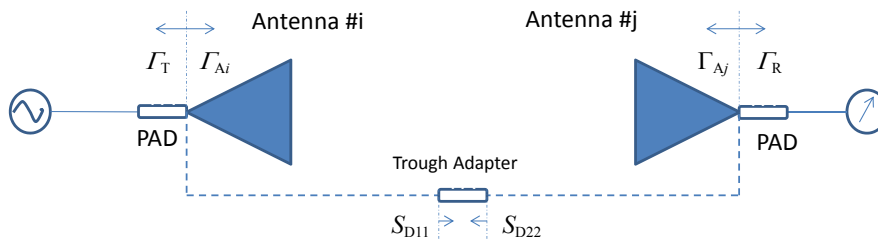


Fig. 6 Reference plane for horn antenna calibration

Table 1 Uncertainty budget of horn antenna calibration by TAM

Source	Probability distribution	Uncertainty (dB)							
		Band#1	Band#2	Band#3	Band#4	Band#5	Band#6	Band#7	Band#8
Ud (Combined): Uncertainty in Antenna Separation Distance		0.072	0.066	0.043	0.057	0.039	0.070	0.048	0.051
(1)Ud1: Uncertainty in Antenna Separation Distance Measurement	Rectangle	0.003	0.003	0.003	0.003	0.003	0.003	0.003	0.003
(2)Ud2: Uncertainty in Antenna Phase Center Position	Rectangle	0.125	0.115	0.075	0.099	0.068	0.121	0.083	0.089
UR (Combined): Uncertainty in Receiving Power Measurement		0.075	0.109	0.106	0.102	0.104	0.169	0.283	0.301
(1)UR1: Uncertainty due to Coaxial Cable Bending	Rectangle	0.010	0.010	0.010	0.010	0.010	0.010	0.010	0.025
(2)UR2: Uncertainty due to Time Variability of Measurement Instrument	Rectangle	0.050	0.050	0.050	0.050	0.050	0.050	0.050	0.050
(3)UD2: Uncertainty due to Temperature Variation of Measurement Instrument	Rectangle	0.030	0.030	0.030	0.030	0.030	0.030	0.030	0.030
(4)UR4: Uncertainty due to Nonlinearity of Receiver	Rectangle	0.040	0.040	0.040	0.040	0.040	0.050	0.050	0.050
(5)UR5: Uncertainty due to Receiver Indicator Resolution	Rectangle	0.005	0.005	0.005	0.005	0.005	0.005	0.005	0.005
(6)UR6: Uncertainty due to Far-Field Condition	Rectangle	0.045	0.106	0.049	0.067	0.031	0.181	0.092	0.080
(7)UR7: Uncertainty due to Antenna Horizontal Axis Alignment (± 1 cm)	Rectangle	0.020	0.020	0.020	0.020	0.030	0.040	0.040	0.083
(8)UR8: Uncertainty due to Antenna Vertical Axis Alignment (± 1 cm)	Rectangle	0.040	0.040	0.040	0.040	0.080	0.050	0.070	0.030
(9)UR9: Uncertainty due to Antenna Azimuth Angle Alignment (± 1 degree)	Rectangle	0.010	0.020	0.020	0.030	0.030	0.090	0.120	0.180
(10)UR10: Uncertainty due to Antenna Elevation Angle Alignment (± 1 degree)	Rectangle	0.010	0.010	0.020	0.020	0.030	0.060	0.060	0.150
(11)UR11: Uncertainty due to Antenna Polarity Angle Alignment (± 1 degree)	Rectangle	0.010	0.020	0.010	0.030	0.020	0.030	0.050	0.020
(12)UR12: Uncertainty due to Signal-to-Noise Ratio (S/N)	Normal	0.002	0.002	0.004	0.006	0.009	0.008	0.030	0.028
(13)UR13: Uncertainty due to Reflections from Inside of Fully Anechoic Room	Rectangle	0.045	0.045	0.045	0.045	0.045	0.050	0.050	0.090
(14)UR14: Uncertainty due to Mismatching	U	0.050	0.081	0.113	0.082	0.078	0.112	0.342	0.335
(15)UR15: Measurement Repeatability	Normal	0.043	0.067	0.049	0.071	0.075	0.092	0.137	0.131
UR0 (Combined): Uncertainty in Direct Connection Power Measurement		0.071	0.071	0.071	0.071	0.071	0.073	0.073	0.074
(1)UR01: Uncertainty of Through Adapter	Rectangle	0.1	0.1	0.1	0.1	0.1	0.1	0.1	0.1
Combined Standard Uncertainty [dB]		0.128	0.157	0.146	0.146	0.143	0.224	0.354	0.376
Expanded Uncertainty ($k = 2$) [dB]		0.3	0.4	0.3	0.3	0.3	0.5	0.8	0.8

uncertainties of 0.3 dB and 0.8 dB, respectively, for Band # 1 and Band #8. The result indicates that the uncertainty is likely to grow as the applied frequency goes higher. The largest factor, as clearly shown in the uncertainty budget, is the effect of mismatching. Also, the budget indicates that, in Band #6, the factors related to the antenna shape, such as the antenna phase center position or the far-field condition, contribute to the growth of the uncertainty.

6 Conclusion

In this paper, we described the calibrations of standard horn antennas in the frequency range of 1 to 18 GHz, for which we have been providing calibration services. We estimated the calibration uncertainties due to applying the TAM as follows: 0.3 dB for Band #1 (1 GHz) and 0.8 dB for Band #7 and 8 (8 to 18 GHz). The results of our actual calibrations so far have shown good calibration stability, supporting the estimation shown above. With regard to the calibration services in 1 to 18 GHz standard horn antennas, we have started calibration services for double ridged guide antenna (DRGA) in addition to the type of antennas for which we have provided services so far. Also, we have a plan to provide our services mainly for DRGAs.

References

- 1 H. Masuzawa, K. Harima, T. Morikawa, and T. Teshima, "Calibration System for 1-5 GHz-band Field Strength Meters," Review of CRL, pp.73-81, June 1993. (in Japanese)
- 2 M. Sakasai, H. Masuzawa, K. Fujii, A. Suzuki, K. Koike, and Y. Yamanaka, "Evaluation of Uncertainty of Horn Antenna Calibration with the Frequency range of 1 GHz to 18 GHz," Journal of NICT, vol.53, no.1, pp.29-42, March 2006.
- 3 Y. Mushiake, "Antennas and Radio Propagation," Corona Publishing, Feb. 1961. (in Japanese)
- 4 IECE, Antenna Engineering Handbook, Ohmsha, p.440, Oct. 1980.
- 5 L. A. Harris, F. L. Warner, "Re-examination of mismatch uncertainty when measuring microwave power and attenuation," IEE Proc., vol.128, Pt. H, no.1, Feb. 1981.



Kojiro SAKAI

Technical Expert, Electromagnetic Compatibility Laboratory, Applied Electromagnetic Research Institute Calibration of Measuring Instruments and Antennas for Radio Equipment



Tsutomu SUGIYAMA

Senior Researcher, Electromagnetic Compatibility Laboratory, Applied Electromagnetic Research Institute Calibration of Measuring Instruments and Antennas for Radio Equipment



Kouichi SEBATA

Senior Researcher, Electromagnetic Compatibility Laboratory, Applied Electromagnetic Research Institute Calibration of Measuring Instruments and Antennas for Radio Equipment, geodesy



Katsumi FUJII, Dr. Eng.

Research Manager, Electromagnetic Compatibility Laboratory, Applied Electromagnetic Research Institute Calibration of Measuring Instruments and Antennas for Radio Equipment, Electromagnetic Compatibility



Iwao NISHIYAMA

Electromagnetic Compatibility Laboratory, Applied Electromagnetic Research Institute Calibration of Measuring Instruments and Antennas for Radio Equipment